PHILOSOPHICAL TRANSACTIONS A

rsta.royalsocietypublishing.org

Review

Cite this article: Willner AE *et al*. 2017 Recent advances in high-capacity free-space optical and radio-frequency communications using orbital angular momentum multiplexing. *Phil. Trans. R. Soc. A* **375**: 20150439.
http://dx.doi.org/10.1098/rsta.2015.0439

Accepted: 13 October 2016

One contribution of 14 to a theme issue 'Optical orbital angular momentum'.

Subject Areas:
electrical engineering, optics

Keywords:
orbital angular momentum, space division multiplexing, free-space optical communications, millimetre-wave communications

Author for correspondence:
Alan E. Willner
e-mail: willner@usc.edu

Recent advances in high-capacity free-space optical and radio-frequency communications using orbital angular momentum multiplexing

Alan E. Willner[1], Yongxiong Ren[1], Guodong Xie[1], Yan Yan[1], Long Li[1], Zhe Zhao[1], Jian Wang[2], Moshe Tur[3], Andreas F. Molisch[1] and Solyman Ashrafi[4]

[1]Department of Electrical Engineering, University of Southern California, Los Angeles, CA 90089, USA
[2]Wuhan National Laboratory for Optoelectronics, School of Optical and Electronic Information, Huazhong University of Science and Technology, Wuhan 430074, Hubei, People's Republic of China
[3]School of Electrical Engineering, Tel Aviv University, Ramat Aviv 69978, Israel
[4]NxGen Partners, Dallas, TX 75219, USA

AEW, 0000-0002-7339-4376

There is a continuing growth in the demand for data bandwidth, and the multiplexing of multiple independent data streams has the potential to provide the needed data capacity. One technique uses the spatial domain of an electromagnetic (EM) wave, and space division multiplexing (SDM) has become increasingly important for increased transmission capacity and spectral efficiency of a communication system. A subset of SDM is mode division multiplexing (MDM), in which multiple orthogonal beams each on a different mode can be multiplexed. A potential modal basis set to achieve MDM is to use orbital angular momentum (OAM) of EM waves. In such a system, multiple OAM beams each carrying an independent data stream are multiplexed at the transmitter, propagate through a common medium and are demultiplexed

THE ROYAL SOCIETY PUBLISHING

at the receiver. As a result, the total capacity and spectral efficiency of the communication system can be multiplied by a factor equal to the number of transmitted OAM modes. Over the past few years, progress has been made in understanding the advantages and limitations of using multiplexed OAM beams for communication systems. In this review paper, we highlight recent advances in the use of OAM multiplexing for high-capacity free-space optical and millimetre-wave communications. We discuss different technical challenges (e.g. atmospheric turbulence and crosstalk) as well as potential techniques to mitigate such degrading effects.

This article is part of the themed issue 'Optical orbital angular momentum'.

1. Introduction

Free-space communication links are important in many data transfer applications, and they can use either optical or radio-frequency (RF) waves [1,2]. However, as the demand for data increases, there is a keen interest in increasing the data capacity of such communication systems [3]. In the past, the capacity of a communication system can be dramatically increased by multiplexing and simultaneously transmitting multiple independent data streams [4,5]. This can be achieved by using various properties of the electromagnetic (EM) wave, including time, wavelength and polarization, such that multiple data streams can be efficiently multiplexed and demultiplexed using appropriate device technologies [3,6,7]. Meeting future bandwidth demands may require new forms of data channel multiplexing [8–10].

One approach that has recently attracted wide interest is to use the spatial property of an EM wave, such that different spatial waves are multiplexed (i.e. space division multiplexing (SDM)) [9]. A special case of SDM is the utilization of orthogonal spatially overlapping and co-propagating spatial modes, known as mode-division multiplexing [8]. In such a system, multiple data channels each identified by a different spatial mode can be efficiently multiplexed at the transmitter and separated at the receiver. Consequently, the system transmission capacity and spectral efficiency (i.e. bits per second per hertz) could be increased by a factor equal to the number of transmitted spatial modes [11,12].

One orthogonal spatial modal basis set that could be used for SDM is orbital angular momentum (OAM) [13,14]. An EM wave carrying OAM has a helical transverse phase of the form $\exp(i\ell\emptyset)$, where $\emptyset$ is the azimuthal angle and ℓ, the OAM charge, is an unbounded integer (with either negative or positive signs) that represents the number of 2π phase changes in the azimuthal direction [15]. Owing to the helical phase structure, an OAM beam has a ring-shaped intensity profile with a central null, and its wavefront twists along the propagation direction with a twisting rate depending on ℓ [16]. OAM beams with different ℓ values are mutually orthogonal [16], so that beams carrying different OAMs can act as independent channel carriers for efficiently (de-)multiplexing multiple information-bearing signals [11]. Moreover, owing to the fact that the OAM spatial domain is independent of other properties of an EM wave, OAM multiplexing is in principle compatible with other existing multiplexing techniques, such as frequency or wavelength division multiplexing (FDM or WDM), and polarization division multiplexing (PDM) [17,18]. Specifically, beams with the same wavelength and polarization can be re-used by applying different OAM chargers to each of the many beams, enabling a potentially significant increase in the system transmission capacity.

Applying OAM to enhance classical communication systems has been quite interesting, and it is especially exciting given that this is the 25th anniversary of the renowned paper by Allen, working with Han Woerdman and colleagues at Leiden University in The Netherlands [13]. Using OAM for communications was pioneered to a large extent over a decade ago by the groups of Padgett [9] and Zeilinger [14], and the community of researchers pursuing this area has grown significantly over the past few years. There has been progress in recent years in SDM communication using OAM multiplexing, pushing it towards achieving a higher transmission capacity, longer link distance, link robustness and system design guidelines. In this paper, we

describe these advances in both OAM-based free-space optical (FSO) and RF communications. We also discuss the technical challenges associated with these OAM-based SDM systems and potential mitigation techniques for improving system performance.

2. Space division multiplexing communications using orbital angular momentum beams

In general, any orthogonal spatial modal set that can allow for efficient generation, (de-)multiplexing and detection can be used for SDM [19]. For an SDM system using OAM beams, each channel is identified by an OAM mode with a different ℓ value [20]. As depicted in figure 1*a*, multiple independent data channels, each on a different OAM beam, are spatially combined and the resulting multiplexed OAM beams are then transmitted through a single aperture towards the receiver. After coaxially propagating through the same free-space medium, the arriving beams are collected at the receiver by another aperture, and subsequently demultiplexed and detected for data recovery. It should be noted that an OAM beam diverges approximately as the square root of $|\ell|$ and high-order modes diverge more during propagation [21,22]. Since OAM, as a fundamental property, can be carried by any helical-phased EM waves, including light and radio waves, OAM multiplexing can be thus used in all frequency ranges [23]. As shown in figure 1*b*, the use of OAM multiplexing might have potential applications in scenarios such as data centres and back-haul connections.

Given that OAM multiplexing employs the orthogonality among OAM beams to enable efficient (de)multiplexing, it requires coaxial propagation and reception of the transmitted modes [12]. This suggests that OAM-multiplexed links may require a more precise system alignment than non-OAM, single-beam communication links [24]. To date, most of the OAM-based free-space SDM systems rely on line-of-sight (LOS) connection between the transmitter and receiver [25,26]. We describe below OAM-multiplexed LOS systems at two different frequency ranges: optics and radio waves.

(a) Orbital angular momentum-multiplexed free-space optical communications

In general, one major concern for an FSO system is its link reliability and robustness stemming from harsh time-varying channel conditions, such as fog, rain and atmospheric turbulence [27,28]. In addition to power loss, these channel conditions may distort the transmitted beam, resulting in significant system performance degradations and even link outage. Moreover, these effects may fluctuate over time with wide dynamic ranges in magnitude [29].

Among these conditions, atmospheric turbulence is generally considered a major factor that limits the system performance [29,30]. It is known that inhomogeneity in the temperature and pressure of the atmosphere lead to random variations in the refractive index along the transmission path, and can easily distort the phase front of a light beam [28]. For FSO links using phase-front-sensitive OAM beams, the effects of atmospheric turbulence become more challenging due to the fact that the proper demultiplexing of the received OAM beams depends on their helical phase-front structures [31,32]. Atmospheric turbulence may lead to fluctuations in the power of received OAM channels and inter-modal crosstalk between channels with different OAM values [33]. Under a dynamic turbulent atmosphere, these degradations are slowly time-varying processes with a time scale of the order of milliseconds (generally much longer than the signalling period) [28,34].

(b) Orbital angular momentum-multiplexed radio-frequency communications

LOS RF communications with fixed transmitter and receiver locations is of increasing importance due to its potential in many applications [35,36]. Conventional LOS RF links can use the well-established multiple-input multiple-output technique with multiple spatially separated

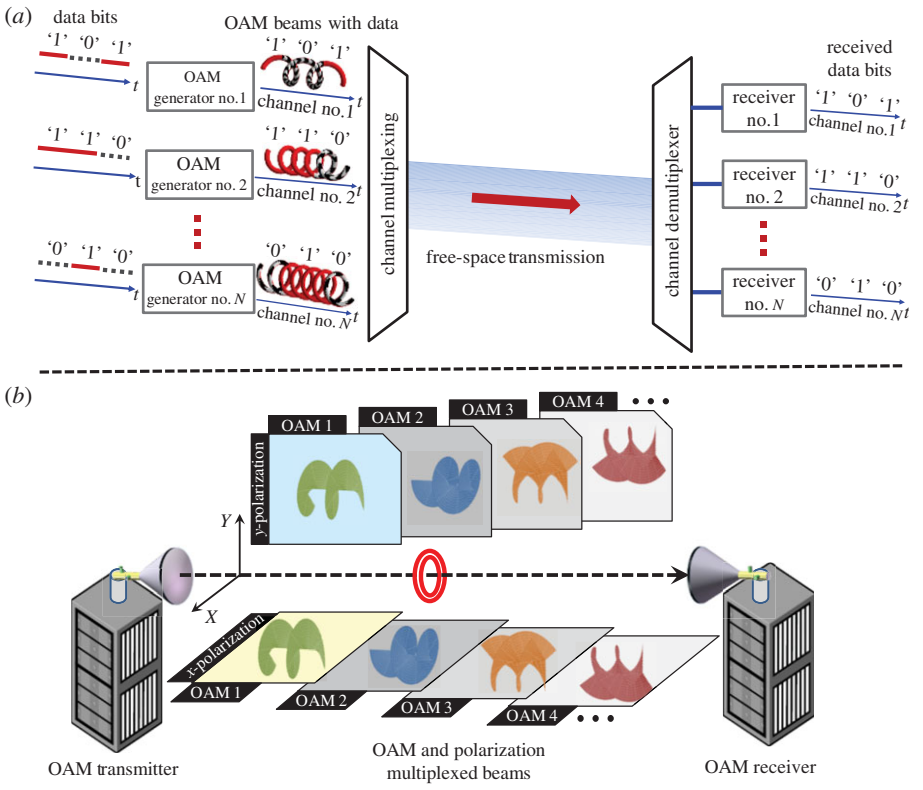

Figure 1. Free-space SDM communication system using OAM beams. (*a*) Multiple OAM beams each carrying an independent data stream can be multiplexed at the transmitter, propagate through free space and be demultiplexed at the receiver. (*b*) Potential application scenarios might include data centres and back-haul connections that require high-capacity data transmission. (Copyright © AAAS 2012 and Macmillan Publishers Ltd 2014.)

aperture elements at the transmitter and receiver for parallel data channel transmission [37]. This technique, called multi-antenna SDM (MA-SDM) systems thereafter, could provide capacity gains relative to the traditional single-aperture systems. In such a system, each data-carrying beam is received by multiple receivers, and signal processing is critical for reducing the crosstalk among channels and thus allow data recovery [38].

LOS RF links can also employ OAM multiplexing for the simultaneous transmission of multiple data channels. An OAM-multiplexed link in the RF regime has a similar concept to that at optical frequencies by multiplexing and transmitting multiple radio OAM waves through a single aperture [11,39]. This approach is different from conventional MA-SDM systems, because it employs OAM beam orthogonality to minimize inter-channel crosstalk and achieve efficient demultiplexing, thus reducing the need for multi-channel signal processing to mitigate channel interferences. Compared with an optical beam, the much longer wavelength of a radio carrier wave suggests less sensitivity to various channel conditions and more divergence upon propagation [21]. Consequently, atmospheric turbulence is not likely to pose severe limitations for this frequency range. On the other hand, the significantly increased divergence of radio OAM waves might impose constraints on the achievable link distance for OAM-multiplexed RF communications.

3. Orbital angular momentum-multiplexed free-space optical communications

The idea of using OAM modes for FSO communications was first proposed and demonstrated by Gibson *et al*. in 2004 [9]. It was shown that OAM modes can be used for data encoding by

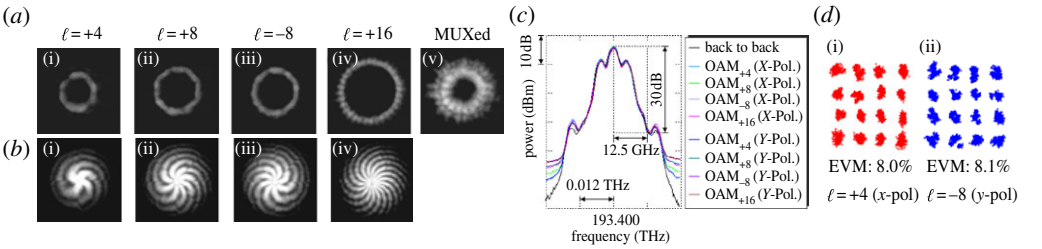

Figure 2. Experimental results of 16-QAM signals over four polarization (Pol.) multiplexed (MUXed) OAM beams [10]. (*a*) Intensity profiles of the four generated OAM beams with $\ell = +4, +8, -8$ and $+16$ and their superposition; (*b*) measured interferograms corresponding to OAM beams with $\ell = +4, +8, -8$ and $+16$; (*c*) measured spectra of each channel after demultiplexing; (*d*) constellations of received 16-QAM signals for channels $\ell = +4$ on *x*-polarization and $\ell = -8$ on *y*-polarization. (Copyright © Macmillan Publishers Ltd 2014.)

sequentially transmitting a different OAM beam, each representing a data symbol, within each time slot. Researchers later realized that each beam can also act as a channel carrier and a group of orthogonal OAM beams can be used to spatially multiplex multiple data streams [18,19]. Recently, high-capacity system transmission results using OAM beams performed under laboratory and field environments or in the field have been reported [10,17,18,40]. Meanwhile, significant efforts have also been made to meet the challenges that hinder its future implementations, pushing towards a high-capacity, long-distance OAM-based FSO link affected by practical atmospheric turbulence conditions [41,42].

(a) High-capacity orbital angular momentum-multiplexed transmission

Initial demonstrations were carried out in the laboratory, including the transmission of two multiplexed beams with each carrying an on–off keying signal [19,20]. Later experiments further showed the possibility of multiplexing and transmitting more OAM modes. In 2011, Wang *et al*. [43] first reported a terabit per second free-space link by combining OAM multiplexing with polarization multiplexing. Four OAM beams on each of two orthogonal polarizations were spatially combined and the resulting multiplexed eight OAM modes then co-axially propagated over approximately 1 m in free space. The received OAM beams were de-multiplexed at the receiver and sequentially detected to recover the data streams. Each of the beams was encoded with a 42.8 GBd 16-quadrature amplitude modulation (16-QAM) signal, allowing a total capacity of approximately 1.4 ($42.8 \times 4 \times 4 \times 2$) Tbit s^{-1}. All eight OAM data channels were located on the same wavelength, providing a spectral efficiency of 25.6 bit s^{-1} Hz^{-1} [10]. Figure 2 presents some of the experimental results.

The above experiment was expanded by adding the wavelength dimension, simultaneously using OAM, polarization and wavelength for multiplexing. A total of 1008 data channels were carried by 12 OAM values, two polarizations and 42 wavelengths [17]. Each channel was encoded with 50 GBd quadrature phase-shift keying, providing an aggregate capacity of 100.8 Tbit s^{-1} ($12 \times 2 \times 42 \times 50 \times 2$ Gbit s^{-1}). Another study [18] further pushed the link capacity beyond petabits per second by multiplexing more OAM channels and using higher order modulation formats.

These free-space OAM system demonstrations attempted to approximate an OAM-carrying Laguerre–Gaussian (LG) beam and used OAM beams with different ℓ. As an LG beam has two indices (i.e. an azimuthal index ℓ related to OAM and a radial index p related to the radial nodes), LG modes can form an orthogonal and complete modal set. OAM does exist for LG modes with higher values of p and OAM beams with higher p indices can also be included for multiplexing, as has been shown in various reports [44,45].

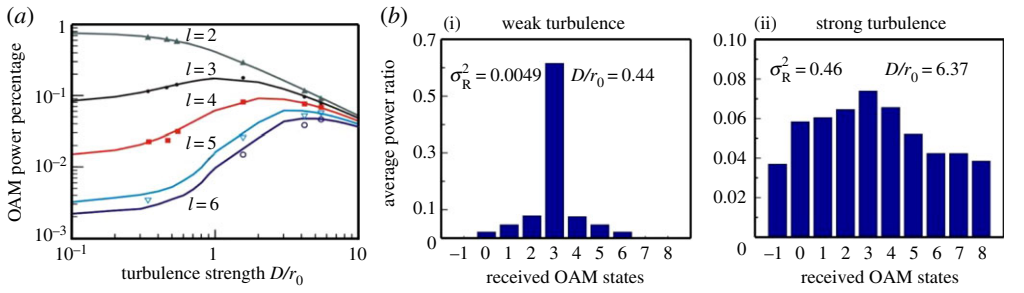

Figure 3. (*a*) The normalized average power in detected modes as a function of turbulence strength D/r_0 for an input mode $\ell = +2$, and (*b*) measured OAM power spectrum when an OAM beam with $\ell = +3$ propagating through the emulated weak and strong turbulence [34]. The Rytov variance σ_R^2 and D/r_0 of the emulated turbulence are also provided. (Copyright © OSA2013.)

(b) Atmospheric turbulence effects and turbulence mitigations for orbital angular momentum beams

(i) Atmospheric turbulence effects

As described in §2a, atmospheric turbulence presents a critical challenge to OAM-based FSO links by giving rise to fluctuations in power and inter-model crosstalk among the received OAM channels [46]. Theoretical works performed by Paterson [31] and Tyler & Boyd [32] provided the quantitative analysis on the effects of atmospheric turbulence on OAM beams, considering the typical Kolmogorov spectrum statistics model. It was revealed that the amount of power of the transmitted OAM modes that leaked into neighbouring modes is proportional to the strength of turbulence D/r_0, where D is the beam width and r_0 is the atmospheric coherence length [28]. Specifically, the ensemble average of the normalized power on the OAM mode $\ell = \ell_j$, $\langle P_j \rangle$, when transmitting the OAM mode ℓ_i can be approximated by [32]:

$$\langle P_j \rangle = \begin{cases} 1 - 1.01\left(\dfrac{D}{r_0}\right)^{5/3} & \text{for } \Delta = 0 \\ 0.142\dfrac{\Gamma(\Delta - 5/6)}{\Gamma(\Delta + 11/6)}\left(\dfrac{D}{r_0}\right)^{5/3} & \text{otherwise,} \end{cases} \tag{3.1}$$

where $\Delta = |i - j|$ and $\Gamma(\cdot)$ is the gamma function. This expression predicts that, as the turbulence strength increases, the power of the transmitted OAM mode starts to leak to neighbouring modes and tends to be equally distributed among modes for strong turbulence. This power leakage behaviour was also experimentally verified in [47] by emulating turbulence with controllable strength in the laboratory. As an example, figure 3 shows the measured OAM power spectrum of the received beam when transmitting the OAM $\ell = +3$ beam under different turbulence strengths [34]. One can see that the received power is better confined to the transmitted OAM mode under weak turbulence, but it spreads to neighbouring modes as the turbulence strength increases.

Furthermore, the influence of atmospheric turbulence on OAM beams was experimentally investigated from a system perspective by evaluating the system power penalty [34]. In this study, atmospheric turbulence was created by a thin-phase screen plate placed in the middle of the link path. The thin plate had a phase distribution obeying Kolmogorov spectrum statistics with a specific r_0, and was mounted on a rotation stage to simulate the turbulence dynamic nature. The strength of the emulated turbulence could be varied by using a plate with a different r_0 or by adjusting the size of the beam that was incident on the plate. It was found that the power penalty may exceed 10 dB under a weak-to-medium turbulence condition and link outage may occur under strong turbulence.

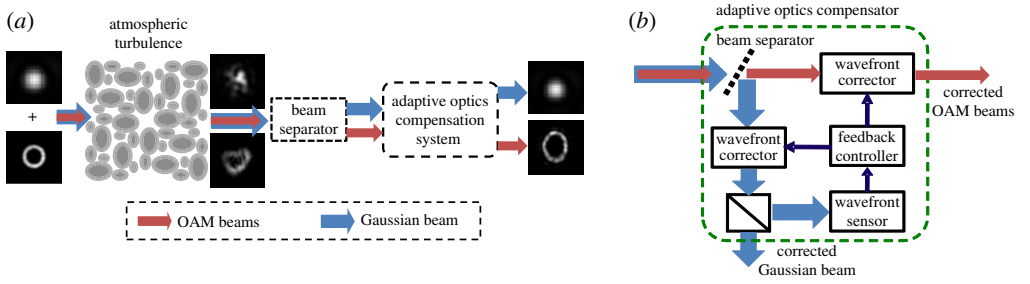

Figure 4. (*a*) Schematic of an AO compensation system for OAM beams, and (*b*) detailed implementation of the AO system [47,48]. It mainly consists of a wavefront measurement unit (e.g. Shack–Hartmann wavefront sensor), two wavefront correctors and a feedback controller. (Copyright © OSA 2014 and 2015.)

(ii) Mitigating turbulence effects

Given the performance degradations described above, it would be desirable to have techniques to mitigate the turbulence effects [48]. Currently, the reported turbulence mitigation approaches can be generally divided into two categories: (i) adaptive optics (AO) system compensation that can help optically correct the distorted wavefronts of received OAM beams [49–51] and (ii) signal processing-based mitigation that employs algorithms in the electrical domain at the receiver to reduce the signal degradation effects [52–54].

AO compensation. In general, an AO compensation system operates in a closed-loop configuration and its one typical working iteration includes: (i) measuring the wavefront of the distorted beams, (ii) calculating the correction patterns based on the wavefront measurement results, and (iii) applying the correction patterns onto the beams to undo the distortions. As for an FSO system using helical phased OAM beams, it is challenging to directly measure an OAM beam's wavefront using conventional wavefront sensors due to its inherent phase singularity [55]. Moreover, it is required that the receiver's AO system should be able to simultaneously compensate multiple coaxially propagating OAM beams.

An AO system that uses a separate Gaussian beam to probe turbulence-induced wavefront distortions was recently proposed to overcome these problems [49]. As depicted in figure 4*a*, a Gaussian beam coaxially propagates with the OAM beams through the turbulent atmosphere. At the receiver, this Gaussian beam is separated from the distorted OAM beams for wavefront measurements, based on which the required phase correction patterns can be derived to undo the distortions of all the received OAM beams. The detailed implementation of the AO system is shown in figure 4*b*. Figure 5 shows the measured intensity profiles of OAM beams and bit error rate (BER) curves before and after compensation. For the convenience of beam separation, the Gaussian beam was orthogonally polarized with respect to the other OAM beams. One can clearly observe that the distorted OAM beams up to $\ell = +9$ were partially corrected, and the power penalty decreased due to the crosstalk reduction by compensation.

Although this Gaussian probe can also carry an independent data channel, its occupation of one polarization sacrifices the polarization degree of freedom for multiplexing. This issue could be avoided by putting the Gaussian probe on a separate wavelength for turbulence sensing, as described in [50]. It was found that the compensation performance degraded slowly with the increase in the beacon's wavelength offset, in the 1520–1590 nm band, from the OAM beams.

Signal processing-based mitigation. Signal processing algorithms in the receiver can also be used to help combat turbulence effects on OAM-based FSO systems. This type of mitigation approach can shift the complexity of the optical subsystem to the electrical domain, providing a complementary approach to AO-based compensation. In [52], a multi-channel equalization algorithm was implemented in the receiver digital signal processing (DSP) to reduce the crosstalk effects caused by weak turbulence and recover all the data channels in a four-OAM-mode multiplexed link. This approach has been previously used in few-mode and multi-mode

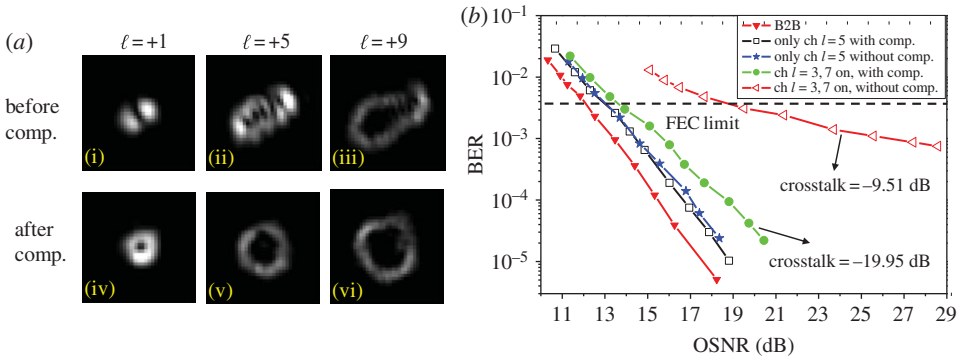

Figure 5. (*a*) Intensity profiles of OAM beams with $\ell = +1, +5$ and $+9$ for a random turbulence realization, and (*b*) BER curves for one OAM channel ($\ell = +5$) when OAM channels $\ell = +1, +5$ and $+7$ were transmitted with and without compensation. FEC, forward error correction; OSNR, optical signal-to-noise ratio. (Reproduced from [47] © OSA 2014.)

fibre-based mode division multiplexed systems to mitigate the mode coupling effects [8]. Experimental results showed that this DSP-based multi-channel equalization can improve the BERs of the received channels and reduce system power penalties.

However, multi-channel equalization is not universally useful for all channel conditions [52,56]. Particularly, outage may occur under strong turbulence distortions when the crosstalk among OAM channels exceeds a certain threshold or one of the channels is barely detectable due to severe power fading [56]. A modified scheme was reported to relieve this concern, through the incorporation of additional OAM transmitters/receivers to create redundancy [53]. By exploiting the spatial diversity provided by the multiple-aperture architecture, both weak and strong turbulence can be potentially mitigated using multi-channel equalization combined with a diversity reception strategy.

Other signal processing approaches that have been shown to help mitigate turbulence effects in OAM-based FSO links, include the Gerchberg–Saxton algorithm [57], artificial neural network-based recognition [54] and the stochastic parallel gradient descent algorithm [58].

(c) Orbital angular momentum-based free-space optical links beyond laboratory distances

The laboratory demonstrations of OAM-multiplexed FSO links were generally limited to a metre-scale short distance. The expansion of an OAM link over a much longer distance might give rise to several issues, including divergences of OAM beams with different orders, system pointing and misalignment, and atmospheric turbulence effects [40,59]. The transmission of OAM beams over a 3 km link across the city of Vienna was reported by Zeilinger's group in Austria [54]. In this experiment, the data bits were sequentially transmitted at a rate of a few bits per second on one of 16 different OAM superposition states ($\ell = \pm 0, \pm 1, \ldots \pm 15$). An artificial neural network algorithm was used to distinguish the received mode-intensity patterns, thus recovering the encoded bit information. This experimental scheme was recently extended to a link distance of 143 km between the two Canary Islands of La Palma and Tenerife [60]. Figure 6 shows the link layout and set-up. The received mode superpositions can be identified with an accuracy of more than 80% up to the third mode order and the decoded message had an error rate of 8.33%. These two long-range experiments indicate the feasibility of kilometre-scale long-distance OAM mode transmission through the atmosphere.

Additionally, the transmission of multiplexed high-speed data-carrying OAM beams was experimentally demonstrated outside the laboratory [40,61]. Ren *et al*. [40] reported a 400 Gbit s^{-1} data link over 120 m by multiplexing four OAM beams with $\ell = -3, -1, +1$ and $+3$. As shown in figure 7, the transmitter and receiver were located at the same site on the roof of

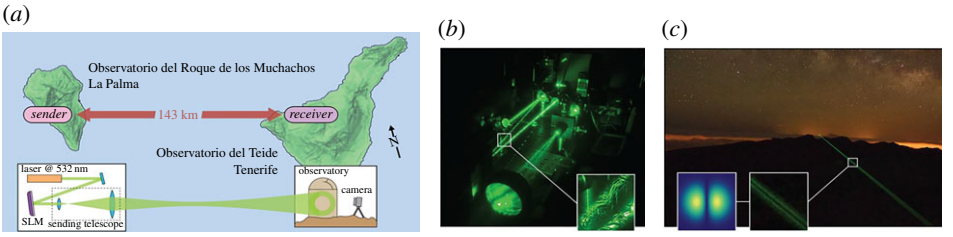

Figure 6. (*a*) Schematic of a 143 km link between two Canary Islands. (*b*) The transmitter located on the Jacobus Kapteyn telescope on the island of La Palma. (*c*) A top-view photo of the link. Data encoding at a few hertz was performed by modulating a spatial light modulator with different phase holograms. The received mode structure at the island of Tenerife was recorded by a regular camera and the encoded data bits were recovered using artificial neural network-based pattern recognition. (Reprinted from [61] © arXiv 2016.)

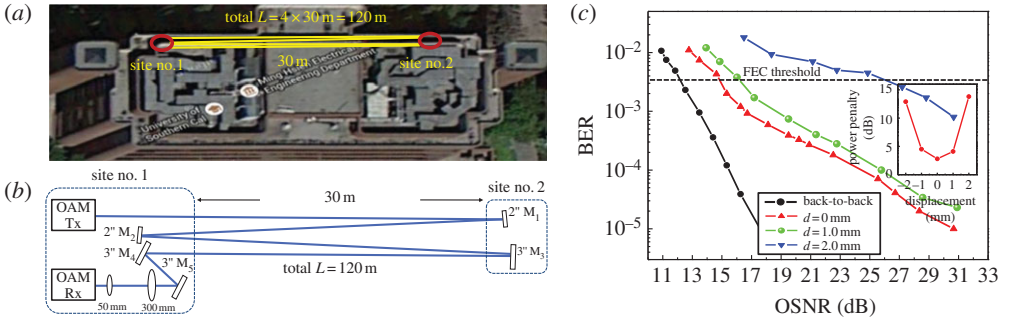

Figure 7. (*a*) Link layout on the building roof and (*b*) transmitter (Tx) and receiver (Rx) geometry. (*c*) Measured BER and system power penalty under various beam displacements for OAM $\ell = +3$ channel [40]. (Copyright © OSA 2016.)

a building. The transmitted OAM beams were reflected twice by two flat mirrors placed 30 m away, achieving a 120 m propagation path. The influence of beam wander (i.e. tip/tilt abreactions) of the link was measured and characterized. Experimental results showed that beam wander significantly degrades the link performance and power penalties increase rapidly when the lateral displacement increases.

(d) Link parameter design for orbital angular momentum-based free-space optical systems

In general, a long-distance FSO system requires a careful design of link parameters. When involving OAM beams, the parameter design of a long-distance link becomes complicated due to their unique intensity and phase profiles [24]. As described in §2, the divergence of OAM beam scales approximately with the square root of $|\ell|$, indicating that high-order modes have a much larger beam size at the receiver. In addition, OAM multiplexing requires coaxial propagation and reception of the transmitted modes. Unlike the case of using a single Gaussian beam, any misalignment between transmitter and receiver apertures or only partially collecting the OAM beams at the receiver would result not only in power loss but, more severely, in inter-channel crosstalk, as presented in figure 8*a*. Figure 8*b* illustrates two types of misalignment: namely lateral misalignment and receiver angular error. These factors need to be carefully considered in the choice of the link parameters of an FSO system using OAM multiplexing.

A simulation model was established in [24] to investigate signal power and crosstalk effects for received OAM channels over pure free-space propagation. The trade-offs between the OAM

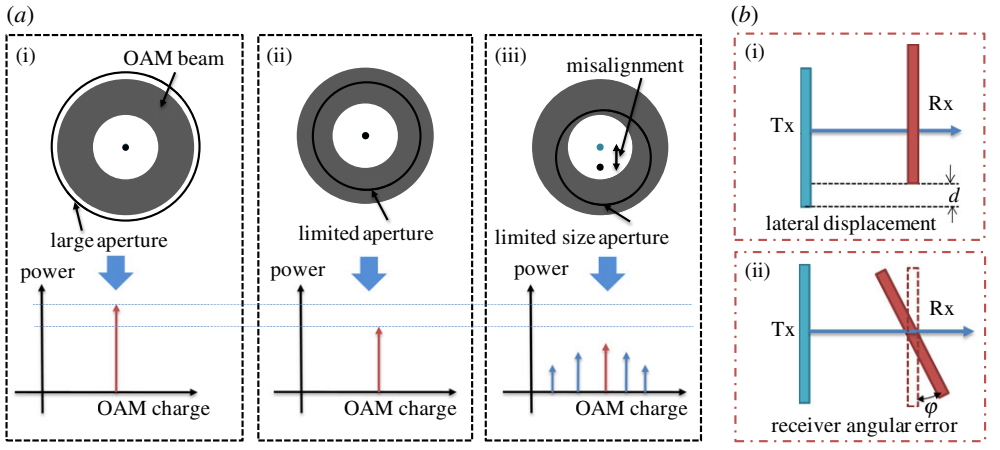

Figure 8. (*a*) Potential challenges for an OAM-multiplexed FSO link: (*a*(i)) receiving an OAM beam with a full receiver aperture and no misalignment; (*a*(ii)) receiving an OAM beam with no misalignment but a limited size aperture; this would only result in the power loss of the detected mode; (*a*(iii)) receiving an OAM beam with misalignment and a limited size aperture; this would cause power leakage onto neighbouring modes. (*b*) Examples of two types of misalignment between the transmitter and receiver: (*b*(i)) lateral displacement and (*b*(ii)) receiver angular error.

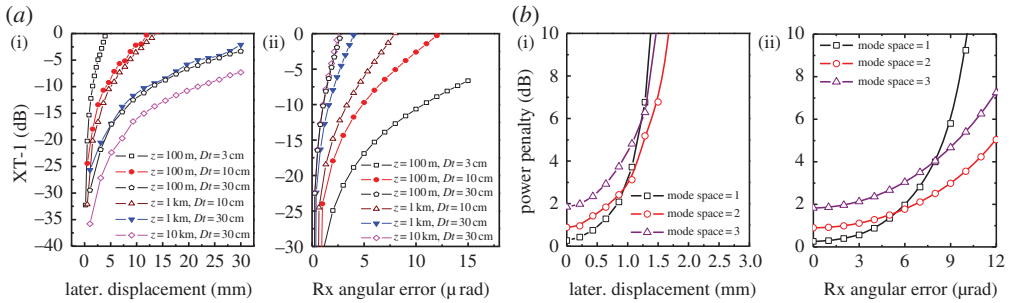

Figure 9. (*a*) Crosstalk to OAM beam $\ell = +4$ as a function of lateral displacement and receiver angular error for different transmission distances *z* and transmitted beam sizes *Dt* when only OAM beam $\ell = +3$ is transmitted. XT-1: relative crosstalk to the adjacent mode OAM beam $\ell = +4$. (*b*) Simulated system power penalty as a function of lateral displacement and receiver angular error when different sets of OAM beams are transmitted over a 100 m link. The transmitted beam size is 3 cm and the receiver aperture size is 4.5 cm. Mode spacing = 1: OAM beams $\ell = +1, +2, +3$ and $+4$ transmitted. Mode spacing = 2: OAM beams $\ell = +1, +3, +5$ and $+7$ transmitted. Mode spacing = 3: OAM beams $\ell = +1, +4, +7$ and $+10$ transmitted. (Reproduced from [24] © OSA 2015.)

modes chosen for transmission, system misalignment tolerance, transmitted beam sizes, aperture sizes and link distance were explored. Based on these trade-offs, design considerations and general guidelines were provided. As an example, figure 9*a* shows misalignment effects on the crosstalk of the adjacent channel $\ell = +4$ under different link distances and transmitted beam sizes when only OAM beam $\ell = +3$ is transmitted. As can be seen from the figure, a larger beam size at the receiver will result in two opposing effects in the cases of lateral misalignment and receiver angular error: (i) a smaller lateral-displacement-induced crosstalk (because the differential phase change per unit area is smaller) and (ii) a larger tilt-phase-error-induced crosstalk (because the phase error scales with a larger optical path delay). Figure 9*b* shows the power penalty analysis for a four-OAM-mode multiplexed link under various lateral displacements and receiver angular errors. It can be found that a system with smaller mode spacing shows a lower system

power penalty under a small lateral displacement or receiver angular error, whereas larger mode spacing shows a lower power penalty when the lateral displacement or receiver angular error is large.

4. Line-of-sight radio-frequency communications using orbital angular momentum beams

OAM can be carried by any EM wave with a helical wavefront, and this does not depend on the carrier-wave frequency. Therefore, OAM multiplexing for communications can be applied to the RF regime. The feasibility of using OAM beams to increase system capacity and spectral efficiency of LOS RF communications is being actively investigated [62,63]. Progress in high-capacity system demonstrations, and in device and component technologies for radio OAM beams, has been also reported [64–67].

(a) High-capacity radio-frequency transmission using orbital angular momentum beams

Although radio OAM waves were first discussed in the late 1990s [68], the use of OAM beams for RF communications has remained relatively unexplored until a few years ago when Tamburini *et al*. [63] reported a data transmission link using OAM beams as data carriers. In this experiment, a Gaussian beam and an OAM beam with $\ell = +1$ at approximately 2.4 GHz were each transmitted by a Yagi–Uda antenna and a spiral parabolic antenna, respectively, which were placed in parallel. These two beams were distinguished by the differential output of a pair of antennas at the receiver side. In a later experiment, the number of channels was increased to three (carried on OAM beams with $\ell = -1$, 0 and $+1$) using a similar apparatus to send an approximately 11 Mbit s^{-1} signal on an approximately 17 GHz carrier [63]. However, different OAM beams in these demonstrations propagate along different spatial axes and were not transmitted through the same aperture. Intensive investigations on OAM-multiplexed RF LOS communications to fully exploit the advantages of OAM modes were performed later, particularly at millimetre-wave (mm-wave) frequencies [64,65].

The proof-of-concept experiment of OAM multiplexing in the RF regime was first demonstrated by Yan *et al*. [11] in a laboratory environment, showing a 32 Gbit s^{-1} mm-wave link at a carrier frequency of 28 GHz. Four different OAM beams with $\ell = -3$, -1, $+1$ and $+3$ on each of two polarizations were generated using spiral phase plates (SPPs) made out of high-density polyethylene. Figure 10*a* presents the observed intensity profile for each of the beams and their interferograms with a Gaussian beam. After spatial combining using specially designed beamsplitters, the resulting eight multiplexed OAM beams propagated over 2.5 m and were then separated at the receiver. All eight OAM channels, each carrying a 1 GBd 16-QAM signal, were sequentially recovered, achieving a capacity of 32 Gbit s^{-1} and a spectral efficiency of approximately 16 bit s^{-1} Hz^{-1} at 28 GHz. As an example, figure 10*b*,*c* shows the recovered 16-QAM constellations and measured BER curves for the two polarized $\ell = +3$ channels.

Later works explored OAM-multiplexed RF communications at other carrier frequencies or using specially designed radio OAM devices [64,65,69]. For example, Li *et al*. [65] reported a 1 Gbit s^{-1} data link at 8.3 GHz by multiplexing two OAM beams with $\ell = +1$ and $+2$, in which two stacked patch antenna arrays were designed and fabricated, and functioned as the OAM transmitter and receiver, respectively. The effects of other channel conditions beyond pure LOS free-space propagation were also investigated recently. Initial studies on the effects of multi-path and object obstructions have been performed [70,71]. As shown in [71], a specular reflection-induced multi-path distorts received OAM beams and causes intra-channel and inter-channel crosstalk, resulting in significant system performance degradations.

Additionally, a similar link design model, as described in §3c, has been applied for mm-wave OAM links to design link parameters and explore potential system limitations [24]. Owing to its much longer wavelength compared with an optical beam, a mm-wave OAM beam diverges more, which would limit the achievable link distance given a fixed-size aperture. Moreover, for

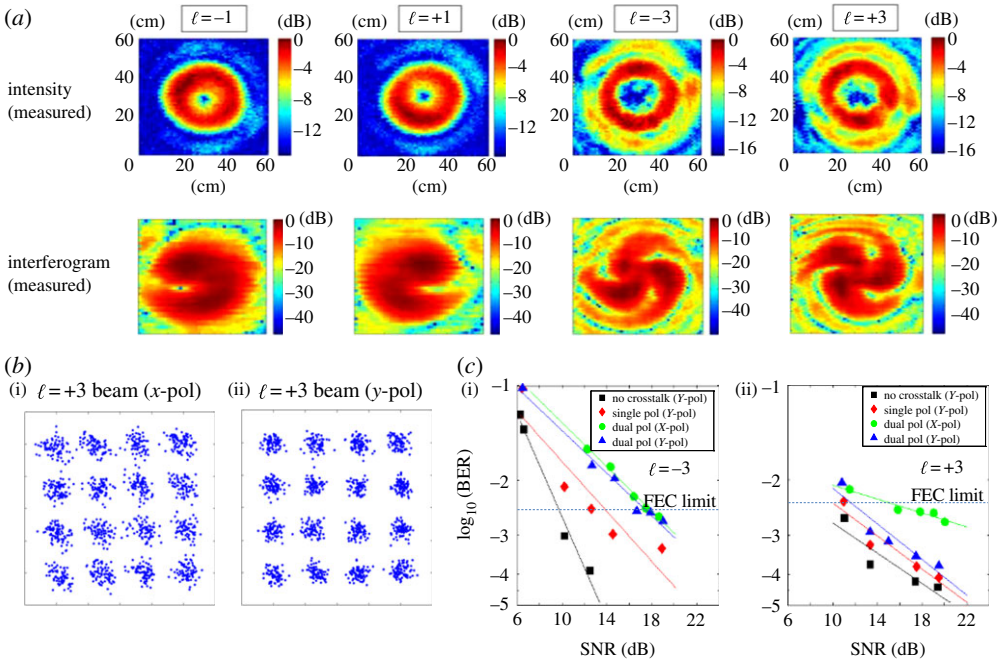

Figure 10. A 32 Gbit s^{-1} data transmission at a 28 GHz carrier frequency by multiplexing eight OAM modes [11]. (*a*) Measured intensity profiles of generated OAM beams and their interferograms. (*b*(i)),(*b*(ii)) Recovered constellations of 4 Gbit s^{-1} 16-QAM signals and (*c*(i))–(*c*(ii)) measured BER curves for $\ell = +3$ channels on each of the two polarizations. SNR, signal-to-noise ratio. (Copyright © Macmillan Publishers Ltd. 2014.)

the same reason, OAM devices at RF generally have larger physical dimensions than those at optical frequencies. These issues together with other features that are specifically related to RF systems, such as the gain and shape of an antenna, should be particularly considered.

(b) Generation and detection of radio orbital angular momentum beams

Various approaches have been put forward to generate, (de-)multiplex and detect radio OAM beams. Turnbull *et al*. [68] first showed the generation of OAM beams at 90 GHz using SPPs made of Teflon. By making use of existing RF components and technologies, other techniques based on different antenna structures have been reported. For example, a helicoidal parabolic antenna was proposed to generate OAM beams with antenna gain [62,63]. Additionally, conventional phase array antennas that have been widely used in RF MA-SDM systems were used for OAM generation by configuring each antenna element with an appropriate phase delay [67]. It was further shown that this approach could also be used for the simultaneous generation and steering of an OAM beam [72,73]. Figure 11*a* presents the concept. By including additional phase delays in the desired steering direction on the eight antenna elements, the generated OAM beam can be steered by up to 30°. As an example, figure 11*b* shows that the measured intensity profiles of steered OAM beam $\ell = +1$ with steering angles of 0°, 5° and 10°.

The generation and multiplexing of multiple OAM beams by a single component has also been investigated [65,69]. By extending the circular patch antenna array approach into a stacked fashion, two multiplexed OAM beams with $\ell = +1$ and $+2$ were generated in a single device fabricated using printed circuit board technology [65]. Moreover, a travelling-wave slot antenna based on a ring cavity resonator and a feeding network was fabricated to produce two co-axially propagating OAM beams with $\ell = -3$ and $+3$ at approximately 94 GHz [64].

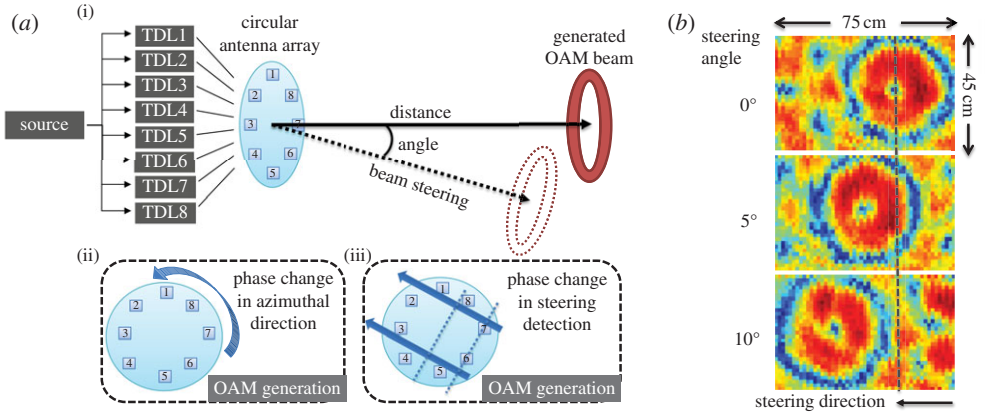

Figure 11. (*a*(i)) The concept of simultaneous generation and steering of an OAM beam using a circular antenna array; (*a*(ii)) phase change in the azimuthal direction for OAM generation; (*a*(iii)) phase change in the steering direction for beam steering. (*b*) The measured intensity profiles of the steered OAM beam $\ell = +1$ with steering angles of 0°, 5° and 10°. (Reproduced from [71] © IEEE 2016.)

(c) Orbital angular momentum multiplexing and multi-antenna space division multiplexing systems

Although OAM multiplexing and the well-established MA-SDM systems represent different implementations, they exploit the spatial degree of freedom for the simultaneous transmission of multiple data channels. There have been intensive discussions as to the fundamental relationship between these two types of spatial multiplexing [74,75]. It was later shown that multi-antenna techniques can be used to generate OAM through suitably structured antenna arrays [67,76]. However, it is also possible to use several spatially separated apertures, each of which contains multiple OAM beams to distribute the spatial degree of freedom, in an arrangement that could be interpreted as combining MA-SDM with OAM multiplexing [77]. It should be noted that a fixed volume that is available for placing transmitter or receiver apertures provides certain spatial degrees of freedom for both multiplexing techniques [78]. An initial experimental demonstration of this concept was reported, in which a 2×2 mm-wave MA-SDM link at 28 GHz with each transmitter containing two OAM beams was implemented [79]. Each of the four OAM channels was encoded with a 1 GBd 16-QAM signal, achieving a total capacity of 16 Gbit s^{-1}. A 4×4 multi-channel signal processing at the receiver was used to mitigate interferences and recover all four data channels [80].

5. Discussion and perspective

Recent years have seen progress in the use of OAM multiplexing for LOS free-space communications in both the optical and RF regimes. There is no doubt that OAM multiplexing, as one SDM approach, can multiply system capacity and spectral efficiency, potentially helping address the capacity demands in many applications. However, there still exists a rich set of issues to further explore for its potential implementation in the future. The following points are worth mentioning:

1. This paper describes using OAM for potentially enhancing capacity in SDM communication systems. There are several issues relating to the OAM modes as well as to other modal groups:
   (a) As long as orthogonality can be maintained among different modes, there exist other modal groups that can also be used for mode multiplexing, e.g. Hermite–Gaussian modes and vector modes [81,82].

(b) As opposed to several other types of modal groups, OAM has circular symmetry. This characteristic makes the beams conveniently matched to many optical components and subsystems for ease of implementation.

(c) OAM beams in this paper can be considered LG modes. In general, LG modes represent a complete two-dimensional modal basis set and can be described by two indices (i.e. an azimuthal index ℓ and a radial index p), and OAM can exist for LG modes with different values of p. If only $p = 0$ is used for multiple beams of different ℓ values, then this can be considered a subset of the fuller two-dimensional set of LG modes [83]. However, as OAM can exist for $p \neq 0$ as well, then the use of different values of p and different ℓ values can produce a fuller set of modes and theoretically a higher system capacity over a given spatial area [44,45].

2. The use of OAM multiplexing under more complicated and harsher channel conditions than described in this paper (e.g. rain, fog and obstructions) remains challenging. It would be important to investigate the system performance under these conditions and develop potential techniques to combat the degradation effects [70].
3. The future of OAM deployment relies heavily on the development of an ecosystem for OAM generation and multiplexing. Currently, most of the reported systems with OAM multiplexing use bulky and expensive components that are not necessarily optimized for OAM operation. The advances in enabling devices, components and subsystems have become critically important [84]. Following the historic trends for many previous advances in communications, it would be essential for the OAM ecosystem to provide reductions in cost and size, and offer compatibility with existing technologies.

Authors' contributions. All the authors contributed to the writing of the manuscript.

Competing interests. The authors declare no competing interests.

Funding. Our work was supported by the Air Force Office of Scientific Research, the DARPA InPho (Information in a Photon) Program, the Intel Labs Research Office, NxGen Partners, the NSF EECS program and the NSF MRI program.

Acknowledgments. The authors acknowledge Prof. Robert W. Boyd, Prof. Ivan B. Djordjevic, Prof. Mark A. Neifeld, Prof. Miles J. Padgett and Prof. Jeffrey H. Shapiro for fruitful discussions.

References

1. Khalighi MA, Uysal M. 2014 Survey on free space optical communication: a communication theory perspective. *IEEE Commun. Surveys Tutorials* **16**, 2231–2258. (doi:10.1109/COMST.2014.2329501)
2. Roh W, Seol J, Park J, Lee B, Lee J, Kim Y, Cho J, Cheun K, Aryanfar F. 2014 Millimeter-wave beamforming as an enabling technology for 5G cellular communications: theoretical feasibility and prototype results. *IEEE Commun. Mag.* **52**, 106–113. (doi:10.1109/MCOM.2014.6736750)
3. Wang C *et al.* 2014 Cellular architecture and key technologies for 5G wireless communication networks. *IEEE Commun. Mag.* **52**, 122–130. (doi:10.1109/MCOM.2014.6736752)
4. Winzer PJ, Essiambre RJ. 2006 Advanced optical modulation formats. *Proc. IEEE* **94**, 952–985. (doi:10.1109/JPROC.2006.873438)
5. Mukherjee B. 2000 WDM optical communication networks: progress and challenges. *IEEE J. Selected Areas Commun.* **18**, 1810–1824. (doi:10.1109/49.887904)
6. Kawanishi S. 1998 Ultrahigh-speed optical time-division-multiplexed transmission technology based on optical signal processing. *IEEE J. Quantum Electron.* **34**, 2064–2079. (doi:10.1109/3.726595)
7. Ciaramella E, Arimoto Y, Contestabile G, Presi M, D'Errico A, Guarino V, Matsumoto M. 2009. 1.28-Tb/s (32×40 Gb/s) free-space optical WDM transmission system. *IEEE Photon. Technol. Lett.* **21**, 1121–1123. (doi:10.1109/LPT.2009.2021149)
8. Richardson DJ, Fini JM, Nelson LE. 2013 Space-division multiplexing in optical fibres. *Nat. Photon.* **7**, 354–362. (doi:10.1038/nphoton.2013.94)

9. Gibson G, Courtial J, Padgett MJ, Vasnetsov M, Pasko V, Barnett SM, Franke-Arnold S. 2004 Free-space information transfer using light beams carrying orbital angular momentum. *Opt. Express* **12**, 5448–5456. (doi:10.1364/OPEX.12.005448)
10. Wang J *et al.* 2012 Terabit free-space data transmission employing orbital angular momentum multiplexing. *Nat. Photonics* **6**, 488–496. (doi:10.1038/nphoton.2012.138)
11. Yan Y *et al.* 2014 High-capacity millimetre-wave communications with orbital angular momentum multiplexing. *Nat. Commun.* **5**, 1–9. (doi:10.1038/ncomms5876)
12. Willner AE *et al.* 2015 Optical communications using orbital angular momentum beams. *Adv. Opt. Photon.* **7**, 66–106. (doi:10.1364/AOP.7.000066)
13. Allen L, Beijersbergen MW, Spreeuw RJC, Woerdman JP. 1992 Orbital angular-momentum of light and the transformation of Laguerre–Gaussian laser modes. *Phys. Rev. A* **45**, 8185–8189. (doi:10.1103/PhysRevA.45.8185)
14. Mair A, Vaziri A, Weihs G, Zeilinger A. 2001 Entanglement of the orbital angular momentum states of photons. *Nature* **412**, 313–316. (doi:10.1038/35085529)
15. Yao AM, Padgett MJ. 2011 Orbital angular momentum: origins, behavior and applications. *Adv. Opt. Photon.* **3**, 161–204. (doi:10.1364/AOP.3.000161)
16. Barnett S, Allen L. 1994 Orbital angular momentum and non paraxial light beams. *Opt. Commun.* **110**, 670–678. (doi:10.1016/0030-4018(94)90269-0)
17. Huang H *et al.* 2014 100 Tbit/s free-space data link enabled by three-dimensional multiplexing of orbital angular momentum, polarization, and wavelength. *Opt. Lett.* **39**, 197–200. (doi:10.1364/OL.39.000197)
18. Wang J *et al.* 2014 N-Dimentional multiplexing link with 1.036-Pbit/s transmission capacity and 112.6-bit/s/Hz spectral efficiency using OFDM-8 QAM signals over 368 WDM pol-muxed 26 OAM modes. In *Proc. of 40th European Conf. on Optical Communication, Cannes, France, 21–25 September 2014*, paper Mo.4.5.1. Piscataway, NJ: IEEE.
19. Awaji Y, Wada N, Toda Y. 2010 Demonstration of spatial mode division multiplexing using Laguerre–Gaussian mode beam in telecom-wavelength. In *Proc. of the IEEE Photonics Conference*, *Denver, Colorado, 7–11 November 2010*, paper WBB2. New York, NY: IEEE.
20. Martelli P, Gatto A, Boffi P, Martinelli M. 2011 Free-space optical transmission with orbital angular momentum division multiplexing. *Electron. Lett.* **47**, 972–973. (doi:10.1049/el.2011.1766)
21. Phillips RL, Andrews LC. 1983 Spot size and divergence for Laguerre Gaussian beams of any order. *Appl. Opt.* **22**, 643–644. (doi:10.1364/AO.22.000643)
22. Padgett MJ, Miatto FM, Lavery MPJ, Zeilinger A, Boyd RW. 2015 Divergence of an orbital-angular-momentum-carrying beam upon propagation. *New J. Phys.* **17**, 1–5. (doi:10.1088/1367-2630/17/2/023011)
23. Thidé B, Then H, Sjoholm J, Palmer K, Bergman J, Carozzi TD, Istomin YN, Ibragimov NH, Khamitova R. 2007 Utilization of photon orbital angular momentum in the low-frequency radio domain. *Phys. Rev. Lett.* **99**, 1–4. (doi:10.1103/PhysRevLett.99.087701)
24. Xie G *et al.* 2015 Performance metrics and design considerations for a free-space optical orbital-angular-momentum multiplexed communication link. *Optica* **2**, 357–365. (doi:10.1364/OPTICA.2.000357)
25. Guan B *et al.* 2004 Free-space coherent optical communication with orbital angular, momentum multiplexing/demultiplexing using a hybrid 3D photonic integrated circuit. *Opt. Express* **22**, 145–156. (doi:10.1364/OE.22.000145)
26. Djordjevic IB. 2011 Deep-space and near-Earth optical communications by coded orbital angular momentum (OAM) modulation. *Opt. Express* **19**, 14 277–14 289. (doi:10.1364/OE.19.014277)
27. Chan VWW. 2006 Free-space optical communications. *IEEE J. Lightw. Technol.* **24**, 4750–4762. (doi:10.1109/JLT.2006.885252)
28. Andrews L, Phillips R. 2005 *Laser beam propagation through random media*, 2nd edn. Bellingham, WA: SPIE.
29. Andrews L, Phillips R, Weeks AR. 1997 Propagation of a Gaussian beam wave through a random phase screen. *Waves Random Media* **7**, 229–244. (doi:10.1088/0959-7174/7/2/005)
30. Nistazakis HE, Tsiftsis TA, Tombras GS. 2009 Performance analysis of free-space optical communication systems over atmospheric turbulence channels. *IET Commun.* **3**, 1402–1409. (doi:10.1049/iet-com.2008.0212)

31. Paterson C. 2005 Atmospheric turbulence and orbital angular momentum of single photons for optical communication. *Phys. Rev. Lett.* **94**, 153901. (doi:10.1103/PhysRevLett.94.153901)
32. Tyler GA, Boyd RW. 2009 Influence of atmospheric turbulence on the propagation of quantum states of light carrying orbital angular momentum. *Opt. Lett.* **34**, 142–144. (doi:10.1364/OL.34.000142)
33. Anguita JA, Neifeld MA, Vasic BV. 2008 Turbulence-induced channel crosstalk in an orbital angular momentum-multiplexed free-space optical link. *Appl. Opt.* **47**, 2414–2429. (doi:10.1364/AO.47.002414)
34. Ren Y *et al.* 2013 Atmospheric turbulence effects on the performance of a free space optical link employing orbital angular momentum multiplexing. *Opt. Lett.* **38**, 4062–4065. (doi:10.1364/OL.38.004062)
35. Chandrasekhar V, Andrews JG, Gatherer A. 2008 Femtocell networks: a survey. *IEEE Commun. Mag.* **46**, 59–67. (doi:10.1109/MCOM.2008.4623708)
36. Halperin D, Kandula S, Padhye J, Bahl P, Wetherall D. 2011 Augmenting data center networks with multi-gigabit wireless links. *Proc. ACM SIGCOMM Computer Commun. Rev.* **41**, 38–49. (doi:10.1145/2043164.2018442)
37. Paulraj A, Gore D, Nabar RU, Bolcksei H. 2014 An overview of MIMO communications—a key to gigabit wireless. *Proc. IEEE* **92**, 198–218. (doi:10.1109/JPROC.2003.821915)
38. Molisch AF. 2011 *Wireless communications*, 2nd edn. New York, NY: Wiley.
39. Mahmouli FE, Walker D. 2013 4-Gbps uncompressed video transmission over a 60-GHz orbital angular momentum wireless channel. *IEEE Wireless Commun. Lett.* **2**, 223–226. (doi:10.1109/WCL.2013.012513.120686)
40. Ren Y *et al.* 2016 Experimental characterization of a 400 Gbit/s orbital angular momentum multiplexed free-space optical link over 120-meters. *Opt. Lett.* **41**, 622–625. (doi:10.1364/OL.41.000622)
41. Ren Y *et al.* 2014 Adaptive-optics-based simultaneous pre- and post-turbulence compensation of multiple orbital-angular-momentum beams in a bidirectional free-space optical link. *Optica* **1**, 376–382. (doi:10.1364/OPTICA.1.000376)
42. Rodenburg B, Mirhosseini M, Malik M, Magaña-Loaiza OS, Yanakas M, Maher L, Steinhoff N, Tyler G, Boyd RW. 2014 Simulating thick atmospheric turbulence in the lab with application to orbital angular momentum communication. *New J. Phys.* **16**, 033020. (doi:10.1088/1367-2630/16/3/033020)
43. Wang J *et al.* 2011 Demonstration of 12.8-bit/s/Hz spectral efficiency using 16-QAM signals over multiple orbital-angular-momentum mode. In *Proc. 37th European Conf. and Exposition on Optical Communications, Geneva, Switzerland, 18–22 September 2011*, paper We.10.P1.76. Piscataway, NJ: IEEE.
44. Xie G *et al.* 2016 Experimental demonstration of a 200 Gbit/s free-space optical link by multiplexing Laguerre Gaussian beams with different radial indices. *Opt. Lett.* **42**, 3447–3450. (doi:10.1364/OL.41.003447)
45. Trichili A, Rosales-Guzmán C, Dudley A, Ndagano B, Salem AB, Zghal M, Forbes A. 2016 Optical communication beyond orbital angular momentum. *Sci. Rep.* **6**, 1–6. (doi:10.1038/srep27674)
46. Anguita JA, Rodriguez HP, Vial MA. 2014 Characterization of OAM states affected by turbulence for high-speed short-range link. *Front. Opt.*, FTh3B.5. (doi:10.1364/FIO.2014.FTh3B.5)
47. Rodenburg B, Lavery MPJ, Malik M, O'Sullivan MN, Mirhosseini M, Robertson DJ, Padgett M, Boyd RW. 2012 Influence of atmospheric turbulence on states of light carrying orbital angular momentum. *Opt. Lett.* **37**, 3735–3737. (doi:10.1364/OL.37.003735)
48. Chandrasekaran N, Shapiro JH. 2014 Photon information efficient communication through atmospheric turbulence–Part I: channel model and propagation statistics. *IEEE J. Lightw. Technol.* **32**, 1075–1087. (doi:10.1109/JLT.2013.2296851)
49. Ren Y *et al.* 2014 Adaptive optics compensation of multiple orbital angular momentum beams propagating through emulated atmospheric turbulence. *Opt. Lett.* **39**, 2845–2848. (doi:10.1364/OL.39.002845)
50. RenY *et al.* 2015 Turbulence compensation of an orbital-angular-momentum and polarization multiplexed link using a data-carrying beacon on a separate wavelength. *Opt. Lett.* **40**, 2249–2252. (doi:10.1364/OL.40.002249)

51. Li S, Wang J. 2016 Compensation of a distorted N-fold orbital angular momentum multicasting link using adaptive optics. *Opt. Lett.* **41**, 1482–1485. (doi:10.1364/OL.41.001482)
52. Huang H *et al.* 2014 Crosstalk mitigation in a free space orbital angular momentum multiplexed communication link using 4 × 4 MIMO equalization. *Opt. Lett.* **39**, 4360–4363. (doi:10.1364/OL.39.004360)
53. Ren Y *et al.* 2016 Atmospheric turbulence mitigation in an OAM-based MIMO free-space optical link using spatial diversity combined with MIMO equalization. *Opt. Lett.* **41**, 2406–2409. (doi:10.1364/OL.41.002406)
54. Krenn M, Fickler R, Fink M, Handsteiner J, Malik M, Scheidl T, Ursin R, Zeilinger A. 2014 Twisted light communication through turbulent air across Vienna. *New J. Phys.* **16**, 113028. (doi:10.1088/1367-2630/16/11/113028)
55. Murphy K, Burke D, Devaney N, Dainty C. 2010 Experimental detection of optical vortices with a Shack-Hartmann wavefront sensor. *Opt. Express* **18**, 15 448–15 460. (doi:10.1364/OE.18.015448)
56. Winzer PJ, Foschini GJ. 2011 MIMO capacities and outage probabilities in spatially multiplexed optical transport systems. *Opt. Express* **19**, 16 680–16 696. (doi:10.1364/OE.19.016680)
57. Ren Y *et al.* 2012 Correction of phase distortion of an OAM mode using GS algorithm based phase retrieval. In *Conf. on Lasers and Electro-Optics* (*CLEO*), *San Jose, CA, 6–11 May 2012*, paper CF3I.4. Washington, DC: OSA Publishing.
58. Xie G *et al.* 2015 Phase correction for a distorted orbital angular momentum beam using a Zernike polynomials-based stochastic-parallel-gradient-descent algorithm. *Opt. Lett.* **40**, 1197–1200. (doi:10.1364/OL.40.001197)
59. Vallone G, Ambrosio V, D'Sponselli A, Slussarenko S, Marrucci L, Sciarrino F, Villoresi P. 2014 Free-space quantum key distribution by rotation-invariant twisted photons. *Phys. Rev. Lett.* **113**, 060503. (doi:10.1103/PhysRevLett.113.060503)
60. Krenn M, Handsteiner J, Fink M, Fickler R. Ursin R, Malik M, Zeilinger A. 2016 Twisted light transmission over 143 kilometers. (http://arxiv.org/abs/1606.01811).
61. Zhao Y, Liu J, Du J, Li S, Luo Y, Wang A, Zhu L, Wang J. 2016 Experimental demonstration of 260-meter security free-space optical data transmission using 16-QAM carrying orbital angular momentum (OAM) beams multiplexing. In *Proc. of Optical Fiber Communication Conf., Anaheim, CA, 20–24 March 2016*, paper Th1H.3. Washington, DC: OSA Publishing.
62. Tamburini F, Mari E, Thide B, Barbieri C, Romanato F. 2011 Experimental verification of photon angular momentum and vorticity with radio techniques. *Appl. Phys. Lett.* **99**, 1–3. (doi:10.1063/1.3659466)
63. Tamburini F, Mari E, Sponselli A, Thidé B, Bianchini A, Romanato F. 2012 Encoding many channels on the same frequency through radio vorticity: first experimental test. *New J. Phys.* **14**, 1–17.
64. Hui X, Zheng S, Chen Y, Hu Y, Jin X, Chi H, Zhang X. 2015 Communication with dual orbital angular momentum (OAM) mode antennas. *Sci. Rep.* **5**, 1–9. (doi:10.1038/srep10148)
65. Li Z, Ohashi Y, Kasai K. 2014 A dual-channel wireless communication system by multiplexing twisted radio wave. In *Proc. of the 44th European Microwave Conf., Rome, Italy, 5–10 October 2014*. Piscataway, NJ: IEEE.
66. Cheng L, Hong W, Hao Z. 2014 Generation of electromagnetic waves with arbitrary orbital angular momentum modes. *Sci. Rep.* **4**, 1–5. (doi:10.1038/srep04814)
67. Tennant A, Allen B. 2012 Generation of OAM radio waves using circular time-switched array antenna. *IET Electron. Lett.* **48**, 1365–1366. (doi:10.1049/el.2012.2664)
68. Turnbull GA, Roberson DA, Smith GM, Allen L, Padgett MJ. 1996 Generation of free-space Laguerre–Gaussian modes at millimetre-wave frequencies by use of a spiral phase plate. *Opt. Commun.* **127**, 183–188. (doi:10.1016/0030-4018(96)00070-3)
69. Zhao Z *et al.* 2016 A dual-channel 60 GHz communications link using patch antenna arrays to generate data-carrying orbital-angular-momentum beams. In *Proc. of IEEE Int. Communications Conf., Kuala Lumpur, Malaysia, 22–27 May 2016*, paper 1570224643. Piscataway, NJ: IEEE.
70. Ahmed N *et al.* 2016 Mode-division-multiplexing of multiple Bessel-Gaussian beams carrying orbital-angular-momentum for obstruction-tolerant free-space optical and millimetre-wave communication links. *Sci. Rep.* **6**, 1–7. (doi:10.1038/srep22082)
71. Yan Y *et al.* 2015 Experimental measurements of multipath-induced intra- and inter-channel crosstalk effects in a millimeter-wave communications link using orbital-angular-momentum

multiplexing. In *Proc. of IEEE Int. Communication Conf., London, UK, 8–12 June 2015*, paper 1570038347. Piscataway, NJ: IEEE.
72. Klemes M, Boutayeb H, Hyjazie F. 2016 Orbital angular momentum (OAM) modes for 2-D beam-steering of circular arrays. In *Proc. of IEEE Canadian Conf. on Electrical and Computer Engineering, Vancouver, BC, Canada, 14–18 May 2016*, pp. 1–5. Piscataway, NJ: IEEE.
73. Xie G *et al.* 2016 Tunable generation and angular steering of a millimeter-wave orbital-angular-momentum beam using differential time delays in a circular antenna array. In *Proc. of IEEE Int. Communications Conf., Kuala Lumpur, Malaysia, 22–27 May 2016*, paper 1570225424. Piscataway, NJ: IEEE.
74. Mohammadi SM, Daldorff LKS, Bergman JES, Karlsson RL, Thide B, Forozesh K, Carozzi TD, Isham B. 2010 Orbital angular momentum in radio—a system study. *IEEE Trans. Antennas Propag.* **58**, 565–572. (doi:10.1109/TAP.2009.2037701)
75. Bai Q, Tennant A, Allen B, Cano E. 2014 Experimental circular phased array for generating OAM radio beams. *IET Electron. Lett.* **50**, 1414–1415. (doi:10.1049/el.2014.2860)
76. Allen B, Tennant A, Bai Q, Chatziantoniou E. 2014 Wireless data encoding and decoding using OAM modes. *IET Electron. Lett.* **50**, 232–233. (doi:10.1049/el.2013.3906)
77. Ren Y *et al.* 2015 Free-space optical communications using orbital-angular-momentum multiplexing combined with MIMO-based spatial multiplexing. *Opt. Lett.* **40**, 4210–4213. (doi:10.1364/OL.40.004210)
78. Zhang Z, Zheng S, Chen Y, Jin X, Chi H, Zhang X. 2016 The capacity gain of orbital angular momentum based multiple-input-multiple-output system. *Sci. Rep.* **5**, 1–11. (doi:10.1038/srep25418)
79. Ren Y *et al.* 2014 Experimental demonstration of 16 Gb/s millimeter-wave communications using MIMO processing of 2 OAM modes on each of two transmitter/receiver antenna apertures. In *Proc. of 2014 IEEE Global Communications Conf., Austin, TX, 8–12 December 2014*, paper 1569944271. Piscataway, NJ: IEEE.
80. YangJ, Werner JJ, Dumont GA. 2002 The multimodulus blind equalization and its generalized algorithms. *IEEE J. Selected Areas Commun.* **20**, 997–1015. (doi:10.1109/JSAC.2002.1007381)
81. Milione G *et al.* 2015 4×20 Gbit/s mode division multiplexing over free space using vector modes and a q-plate mode (de)multiplexer. *Opt. Lett.* **40**, 1980–1983. (doi:10.1364/OL.40.001980)
82. Milione G, Ip E, Li M-J, Stone J, Peng G, Wang T. 2016 Mode crosstalk matrix measurement of a 1 km elliptical core few-mode optical fiber. *Opt. Lett.* **41**, 2755–2758. (doi:10.1364/OL.41.002755)
83. Zhao N, Li X, Li G, Kahn JM. 2015 Capacity limits of spatially multiplexed free-space communication. *Nat. Photon.* **9**, 822–827. (doi:10.1038/nphoton.2015.214)
84. Cai X, Wang J, Strain MJ, Morris BJ, Zhu J, Sorel M, O'Brien JL, Thompson MG, Yu S. 2012 Integrated compact optical vortex beam emitters. *Science* **338**, 363–366. (doi:10.1126/science.1226528)